PROCEEDINGS OF SCIENCE

Experimental neutrino physics: natural beams, reactors and LBL

Barbara Caccianiga*
Dipartimento di Fisica, Università degli Studi e INFN, Milano 20133
E-mail: barbara.caccianiga@mi.infn.it

This review is devoted to experimental neutrino physics carried out using different types of neutrinos: solar, atmospheric, reactor and accelerator neutrinos. It will provide a critical overview of the main characteristics, differences and complementarieties between the most important experiments on neutrino oscillations. It will describe the current "state of the art" of our knowledge of the fundamental neutrino oscillation parameters in the standard three flavour scenario. Finally, it will discuss the strategies adopted by present and future experiments to try and measure some of the still missing pieces of the neutrino puzzle, in particular, mass hierarchy and δ_{CP}.

The European Physical Society Conference on High Energy Physics
22–29 July 2015
Vienna, Austria

*Speaker.

PoS(EPS-HEP2015)025

1. Introduction

Neutrino oscillations have been theoretically suggested by Pontecorvo back in 1958 ([1]), but have been experimentally demonstrated only many years later, with the work on atmospheric neutrinos published by Super-Kamiokande in 1998 [2], followed few years later by the one published by SNO on solar neutrinos [3]. These two results have been awarded the Nobel Prize for physics in 2015. For oscillations to occur, two conditions must be met: 1) mass and propagation eigenstates for neutrinos must not coincide, which implies the existence of a non-trivial mixing matrix which trasforms one into the other; 2) the mass of at least one neutrino must be different from 0. In the standard three neutrino flavour scenario, mixing is determined by a 3x3 unitary matrix (the so-called PMNS matrix) and oscillations are driven by the two squared mass differences Δm^2_{13} and Δm^2_{12}. A common rapresentation of the PMNS matrix is shown below

$$\begin{bmatrix} \nu_e \\ \nu_\mu \\ \nu_\tau \end{bmatrix} = \begin{bmatrix} U_{e1} & U_{e2} & U_{e3} \\ U_{\mu 1} & U_{\mu 2} & U_{\mu 3} \\ U_{\tau 1} & U_{\tau 2} & U_{\tau 3} \end{bmatrix} \begin{bmatrix} \nu_1 \\ \nu_2 \\ \nu_3 \end{bmatrix}$$

where

$$U = \begin{bmatrix} 1 & 0 & 0 \\ 0 & c_{23} & s_{23} \\ 0 & -s_{23} & c_{23} \end{bmatrix} \begin{bmatrix} c_{13} & 0 & s_{13}e^{-i\delta} \\ 0 & 1 & 0 \\ -s_{13}e^{+i\delta} & 0 & c_{13} \end{bmatrix} \begin{bmatrix} c_{12} & s_{12} & 0 \\ -s_{12} & c_{12} & 0 \\ 0 & 0 & 1 \end{bmatrix} \begin{bmatrix} 1 & 0 & 0 \\ 0 & e^{i\phi_1/2} & 0 \\ 0 & 0 & e^{i\phi_2/2} \end{bmatrix}$$

The matrix depends upon three mixing angles θ_{12}, θ_{23} and θ_{13} ($c_{ij} = \cos\theta_{ij}$ and $s_{ij} = \sin\theta_{ij}$), one Dirac CP-violating phase δ_{CP} and two Majorana phases ϕ_1 and ϕ_2 (which are 0 if the neutrino is a Dirac particle). A neutrino of type ν_α can transform into a neutrino of type ν_β if it has an energy $E >> m_\alpha$ and travels a proper distance L in vacuum. The oscillation probability is given by

$$P(\nu_\alpha \to \nu_\beta) = \delta_{\alpha\beta} - 4\sum_{i<j} \mathrm{Re}(U_{\alpha i}U_{\beta j}U^*_{\alpha j}U^*_{\beta i})\sin^2\Delta_{ji} + 8\,\mathrm{Im}(U_{\alpha i}U_{\beta j}U^*_{\alpha j}U^*_{\beta i}) \prod_{i<j} \sin\Delta_{ji} \quad (1.1)$$

where $\Delta_{ji} = \Delta m^2_{ji}\, L/(4E)$, $i, j = 1,2,3$ and $\alpha, \beta = e, \mu, \tau$.

The oscillation probability is modified if neutrinos cross a dense medium, because of coherent forward scattering on electrons. This effect is referred to as Wolfenstein-Mikheyev-Smirnov (MSW) matter effect and can enhance the oscillation probability under particular resonance conditions, which depend on the electron density in the medium, on the neutrino energy, on the fact that we are dealing with neutrinos or anti-neutrinos and on the sign of $\Delta^2 m$. This last dependency makes it possible to exploit matter effects to determine the neutrino mass hierarchy, as will be discussed in Section 3 and 5, devoted to atmospheric and accelerator neutrinos, respectively. Also solar neutrino oscillations are significantly influenced by matter effects as will be discussed in Section 2.

The oscillation parameters can be studied by dedicated experiments which use either natural or artificial neutrino beams with very well-known flavor-composition, spectrum and flux and observe either flavor disappearance or appearance in a detector located at distance L from the source. The ratio between the neutrino energy E and the experiment baseline L sets the region of the oscillation parameters which can be explored. Also, if the experiment is able of measuring the rate at different L/E, oscillation waves can be seen, which greatly enhance sensitivity and confidence in the results. The main contributions to the determination of θ_{12} and Δm^2_{12} have come from solar

neutrino experiments together with the long baseline reactor experiment KamLAND, while short baseline (~ 1 Km) reactor experiments have provided the currently most precise measurement of θ_{13}. The parameters Δm^2_{13} and θ_{23} have been historically determined with atmospheric neutrinos, but currently the most precise measurements come from accelerator neutrinos. A large amount of experimental data has been collected and the oscillation picture is rather complete: we know with fairly good precision the size of the three mixing angles and of the two Δm^2_{12} and Δm^2_{13} squared mass differences. The current best values of the oscillation parameters are summarized in table 1.

In spite of this rather coherent and complete picture, there are several missing parts of the neutrino puzzle: we know that the three neutrino masses are different from each other, but we don't know their absolute values, nor even their relative ordering (mass hierarchy). Oscillation experiments are not sensitive to the absolute neutrino mass scale (which won't be covered in this paper), but can address and will address the problem of neutrino mass hierarchy with different strategies based on atmospheric, reactors or accelerator neutrinos (see Sections 3, 4 and 5).

Another open issue is CP violation in the leptonic sector, which may have important implications on our understanding of baryogenesis and matter/anti-matter asymmetry. The relatively large value of θ_{13} will make this investigation possible with standard accelerator techniques, with no need to invest in new beam technologies (neutrino factories, beta-beam [5]). Accelerator based experiments will be crucial in the determination of δ_{CP} (see Section 5), although they may require some inputs from reactor or atmospheric neutrino experiments to break degeneracies between unknown parameters.

The currently measured value of θ_{23} is consistent with maximal mixing, $\theta_{23} \sim \pi/4$. It is of great interest to determine whether θ_{23} is maximal or not, and if not, whether it is less or greater than $\pi/4$, as it could constrain models of neutrino mass generation. Accelerator neutrino experiments will play a crucial role to break the octant ambiguity, by combining ν_μ disappearance and ν_e appearance results.

Two important open issues won't be covered in this review: the nature of neutrino, Majorana or Dirac, and the possible existence of sterile neutrinos. The former cannot be adressed by oscillation experiments and requires to search for a lepton number violating process like neutrinoless double beta decay. The latter requires short baseline experiments using different types of neutrinos sources (radioactive sources, reactors or accelerators). Both subjects will be covered by another review presented at this conference [4].

2. Solar neutrino experiments

The Sun emits an enormous amount of electron neutrinos which are produced by nuclear reactions occurring in its core. The total flux of these neutrinos on Earth is $\sim 6 \times 10^{10}\ \nu\ \mathrm{cm}^{-2}\ \mathrm{sec}^{-1}$ and their energy spectrum is shown in Fig. 1, left. Solar neutrinos have provided the first experimental hint pointing towards neutrino oscillations (dating back to 1968, with the first Homestake results), although it took more than 30 years for the experimental picture to be fully understood. The driving idea of the first pioneer experiment Homestake was to corroborate the Standard Solar Model by verifying that the Sun does emit neutrinos and by comparing the measured solar neutrino rate with the predicted one: they found a significant deficit of neutrinos with respect to expectations [6]. This puzzling result was confirmed later on by other experiments (Gallex/GNO [7], SAGE

	Value	Best measurement
θ_{12}	$\sim 33^\circ$	$\tan^2\theta_{12} = 0.437^{+0.029}_{-0.026}$ [13]
θ_{23}	$\sim 45^\circ$	$\sin^2\theta_{23} = 0.514^{+0.055}_{-0.056}$ (NH) [30] $\sin^2\theta_{23} = 0.511^{+0.0055}_{-0.0055}$ (IH) [30]
θ_{13}	$\sim 9^\circ$	$\sin^2 2\theta_{13}$=0.084$\pm$0.005 [26]
Δm^2_{12}	$\sim 7.5 \times 10^{-5}$eV^2	$\Delta m^2_{12} = \left(7.58^{+0.19}_{-0.18} \times 10^{-5}\right)$ eV^2 [22]
Δm^2_{23}	$\sim 2.3 \times 10^{-3}$ eV^2	$\Delta m^2_{23} = [2.28\text{-}2.46] \times 10^{-3}$ eV^2 (68% C.L.)N.H. [32] $\Delta m^2_{23} = [2.32\text{-}2.53] \times 10^{-3}$ eV^2 (68% C.L.) I.H. [32]

Table 1: Current best measurements of the oscillation parameters.

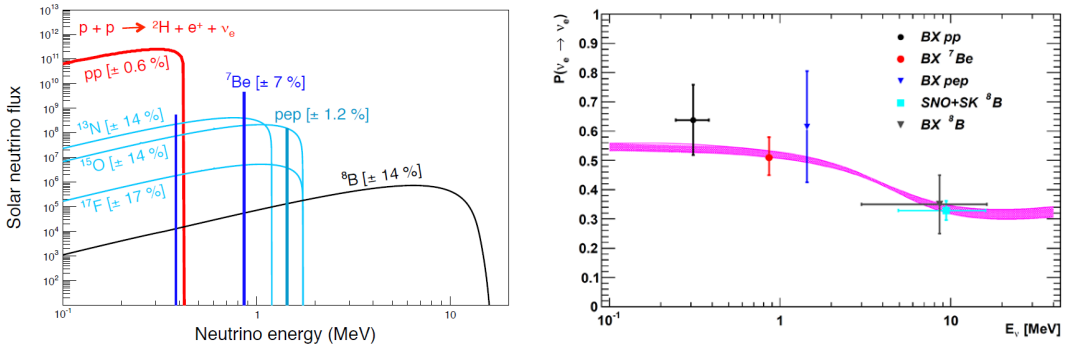

Figure 1: Solar neutrinos. Energy spectrum (left); Survival probability P($\nu_e \to \nu_e$) measured by Borexino, Super-Kamiokande and SNO (right).

[8] and Kamiokande/Super-Kamiokande [9]) opening a 30-year-long scientifical debate which was settled only in 2002 by the results of the heavy-water Cerenkov detector SNO [10]. SNO proved unambiguously that the solution to the "solar neutrino problem" was not to be searched in solar physics, but in neutrino physics, namely, in the quantum mechanics phenomenon of flavour oscillations. Therefore solar neutrino experiments, which were born to study the Sun, turned out to be powerful tools to also study neutrino properties. A large amount of data has been collected on solar neutrinos by Homestake, Gallex, SAGE, Kamiokande/Super-Kamiokande, SNO and more recently by Borexino[11] (which started taking data in 2007 and is still running). All solar neutrino experiments are located underground (where cosmic ray background is small) and feature kton-scale detectors. However, they are based on different techniques (radiochemical, water Cerenkov, liquid scintillator) and have different energy thresholds which makes them sensitive to different portions of the solar neutrino spectrum: the water Cerenkov detectors (Kamiokande, Super-Kamiokande and SNO) are sensitive only to the highest energy neutrinos (the so-called ^{8}B neutrinos), while

radiochemical experiments and Borexino have been able of studying also the lowest energy neutrinos (below 1 MeV). In particular, Borexino has performed a true "spectroscopy" of solar neutrinos by measuring separately the most important components of the solar neutrino flux, namely, the so-called ^{7}Be neutrinos, the pep neutrinos and recently the pp neutrinos which contribute to more than 90% of the solar neutrino flux [14]. Solar neutrino experiments observe electron neutrino disappearance with a characteristic E/L of the order of 10^{-11} eV^2 (E $\sim$ 1 MeV and L $\sim 1.5\times10^{11}$ m), and are mostly sensitive to Δm^2_{12} and θ_{12} (the characteristic oscillation lenght for Δm^2_{13} is small and therefore its contribution is averaged out). Oscillations are enhanced as neutrinos cross the very dense solar matter by the so-called MSW effect which, for the characteristic values of the Sun's density and of Δm^2_{12}, mostly occurs for energies above 1 MeV. This can be clearly seen in Fig. 1, right, where the electron neutrino survival probability is shown as a function of energy. The dots in this plot are obtained by comparing the experimental results with the Standard Solar Model predictions in the high-metallicity hypothesis [12]: while at lower energies the survival probability is around 60% in agreement with the expectations from vacuum-dominated oscillations (P($\nu_e \rightarrow \nu_e$) $\sim$ 1-$\frac{sin^2 2\theta}{2}$), at higher energies the survival probability significantly decreases, because of the resonant effect induced by the solar matter.

A three-flavour analysis of the results from all solar neutrino experiments isolates a relatively small island in the relevant oscillation parameter space θ_{12}, Δm^2_{12} (see Fig. 2). While θ_{12} is well determined by solar neutrino experiments only, Δm^2_{12} is better constrained with the help of KamLAND: this experiment observes anti-neutrinos from reactors (see Section 4) located at an average distance L of $\sim$ 180 Km and has a characteristic E/L $\sim$ 10^{-4} eV^2, well-suited to explore the same region of the solar parameter space . The combination of KamLAND + solar neutrino experiments (assuming CPT invariance) yields to the following best fit values: $\Delta m^2_{12} = \left(7.53^{+0.19}_{-0.18} \times 10^{-5}\right)$ eV^2, $\tan^2\theta_{12} = \left(0.437^{+0.029}_{-0.026}\right)$ and $\sin^2\theta_{13} = \left(0.023^{+0.015}_{-0.015}\right)$ (for details of the globabl analysis see [13]).

Future perspectives for solar neutrino experiments

There is a small tension (2σ) between the results of solar and KamLAND experiments for what concerns Δm^2_{12} (see reference [13]). This tension mainly arises from two facts: 1) the expected up-turn in P($\nu_e \rightarrow \nu_e$) when lowering the energy threshold has not been observed by SNO and Super-Kamiokande; 2) Super-Kamiokande detects a non-vanishing Day/Night asymmetry of the ^{8}B neutrinos flux which disfavors the KamLAND best fit value of Δm^2 for which Earth matter effects are small. Non-standard interactions and super-light sterile neutrinos could modify matter effects and explain this small discrepancy [15]. In order to investigate this possibility, it is important to study the solar neutrino survival probability in the energy region where the transition between vacuum and matter occurs. Both Super-Kamiokande and Borexino will be adressing this issue: Super-Kamiokande will study the up-turn region of the survival probability by further lowering the energy threshold and increasing statistics; Borexino will exploit the enhanced radiopurity of Phase 2 data to improve the measurement of P($\nu_e \rightarrow \nu_e$) for pep and ^{7}Be neutrinos.

3. Atmospheric neutrino experiments

Atmospheric neutrinos are part of the Extensive Air Showers originated by cosmic rays in the Earth atmosphere. They come from the decay of charged pions ($\pi^+ \rightarrow \mu^+\nu_\mu$ and $\pi^- \rightarrow \mu^-\bar{\nu}_\mu$)

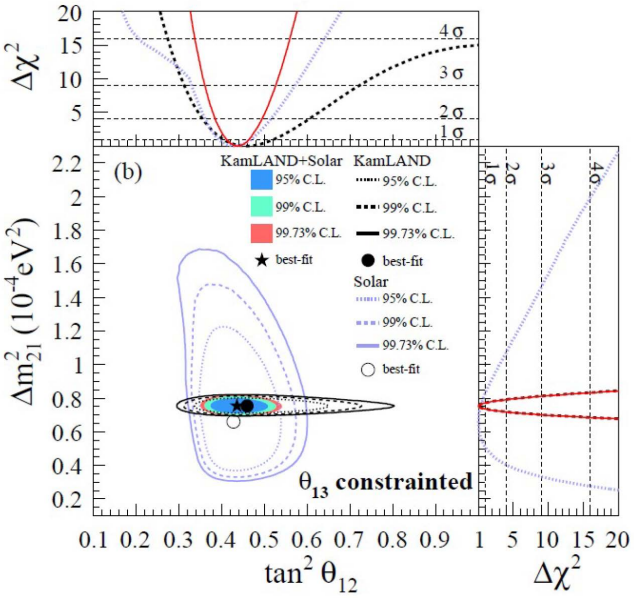

Figure 2: Solar neutrinos. Three -flavour analysis of the results from solar neutrino experiments only (blu curves), KamLAND only (black curves) and solar+KamLAND (solid filled coloured curves) [13].

and of muons ($\mu^+ \to e^+ \bar{\nu}_\mu \nu_e$ and $\mu^- \to e^- \bar{\nu}_e \nu_\mu$) and are therefore a mixture of electron and muon neutrinos (and anti-neutrinos). The average energy of these neutrinos is around 1 GeV, but can extend up to 1 TeV or larger (see Fig. 3, left).

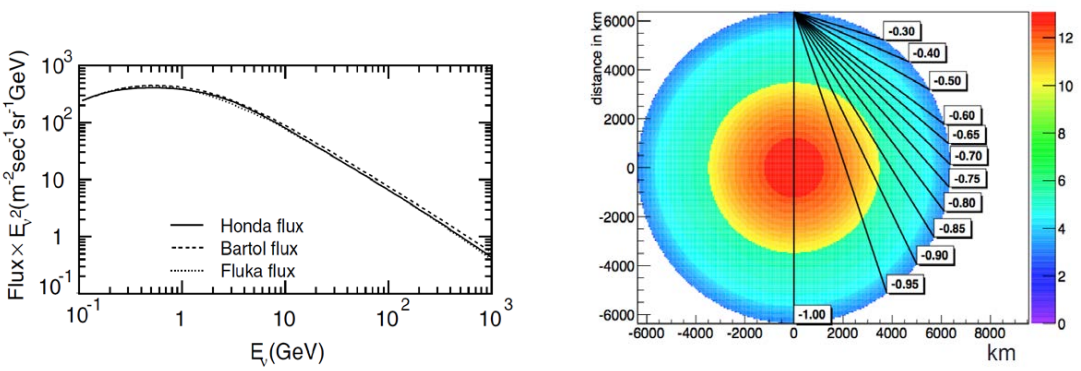

Figure 3: Atmospheric neutrinos. Energy spectrum (left) and distance travelled as a function of the cosθ (right).

Given the fact that ν_μ's are produced both in pion and in muon decays, while ν_e's are produced only in muon decays, muonic type neutrinos are approximately twice as many as electronic type neutrinos. While the absolute number of neutrinos produced in a shower is sensitive to details of the

theoretical models describing the interactions of very high energy particles with the atmosphere, the ratio between the muonic and the electronic component of atmospheric neutrinos is quite robust and almost model independent. The first hint towards atmospheric neutrino oscillations came from the experiments Kamiokande [16] and IMB [17] which observed a deficit in the measured ν_μ to ν_e ratio for upward-going neutrinos. This hint was later confirmed by a detailed analysis of Super-Kamiokande which studied the ν_μ and ν_e fluxes as a function of the zenith angle: selecting different zenith angles is equivalent to selecting different distances travelled by neutrinos before reaching the detector (see Fig. 3, right). The path L varies from $\sim 10^4$ m (for downward-going neutrinos crossing only the Earth atmosphere) to 10^7 m (for upward-going muons crossing the entire Earth diameter) .

Super-Kamiokande confirmed the deficit in the flux of upward-going muon neutrinos and studied the behaviour of this deficit as a function of L/E. They found a pattern which was consistent with the hypothesis of ν_μ flavour conversion with characteristic Δm^2 of the order of $2\times10^{-3}\,\mathrm{eV}^2$. This result was published in 1998 as the first evidence of neutrino oscillations [2]. More recently Super-Kamiokande demonstrated at 3.8σ level that data are compatible with $\nu_\mu \to \nu_\tau$ conversion, ruling out the possibility of oscillations into sterile neutrinos [18].

Future perspectives for atmospheric neutrino experiments

Besides their historical importance, atmospheric neutrinos have recently raised new interest in the scientific community as a possible tool to determine the neutrino mass hierarchy. As described in Section 1, the MSW effect can perturb the oscillatory pattern of neutrinos crossing a dense medium. In particular, in case of atmospheric neutrinos, matter effects can enhance the probability of ν_μ oscillations by sub-leading order terms which increase the ν_μ to ν_e conversion. The ν_μ to ν_e oscillation probability in matter can be approximated by

$$P^M(\nu_\mu \to \nu_e) = P^M(\nu_e \to \nu_\mu) \sim \sin^2\theta_{23}\sin^2 2\theta^m_{13}\sin^2\frac{(\Delta m^2_{13})^m \mathrm{L}}{4E} \tag{3.1}$$

where

$$\begin{aligned} \sin^2 2\theta^m_{13} &= \frac{\sin^2 2\theta_{13}}{\sin^2 2\theta_{13} + \left(\cos 2\theta_{13} - \frac{2AE}{\Delta m^2_{13}}\right)^2} \\ (\Delta m^2_{13})^m &= (\Delta m^2_{13})\sqrt{\sin^2 2\theta_{13} + \left(\cos 2\theta_{13} - \frac{2\sqrt{2}AE}{\Delta m^2_{13}}\right)^2} \end{aligned} \tag{3.2}$$

E is the neutrino energy, A=$+\sqrt{2}\mathrm{G}_F\mathrm{N}_e$, where G_F is the Fermi constant and N_e is the density of electrons in the medium. For anti-neutrinos the oscillation probability $P^M(\bar\nu_\mu \to \bar\nu_e)$ is the same, but with A=$-\sqrt{2}\mathrm{G}_F\mathrm{N}_e$. Matter effects are maximized when the resonance condition is met

$$\Delta m^2_{13}\cos 2\theta_{13} = -2\mathrm{A}\mathrm{N}_e\mathrm{E}$$

For typical values of Earth density, this happens for neutrino energies between 1 and 20 GeV.

Note that the oscillation probability in matter (unlike the one in vacuum) depends on the sign of Δm^2_{13}. Therefore studying matter-induced effects in the oscillation pattern of atmospheric neutrinos can give information on the neutrino mass hierarchy. However, there is some degree of ambiguity, since A and Δm^2_{13} appear together in the oscillation formula in such a way that the same oscillation

pattern is obtained for neutrinos in case of direct (inverse) mass hierarchy and for anti-neutrinos in case of inverse (direct) mass hierarchy: moreover, the resonance condition can be reached by neutrinos only in case of direct hierarchy, while for anti-neutrinos it occurs only in case of inverse mass hierarchy. In principle, to disentangle this ambiguity, one would need to distinguish neutrinos from anti-neutrinos. This is being pursued by the proposed experiment INO which plans to use a 50 kton magnetized iron calorimeter to detect atmospheric neutrinos [19].

Another approach to study mass hierarchy with atmospheric neutrinos is the one exploited by the proposed experiments PINGU [20] and ORCA [21]. These experiments plan to instrument few Mtons of South Pole ice (PINGU) or Mediterranean sea water (ORCA) with strings of photomultiplier tubes, to detect the Cerenkov light emitted by secondary products of atmospheric neutrinos in the medium. This strategy is similar to the the one adopted by the currently running experiment IceCube and by the proposed experiment ARCA (within the KM3NET project), but the granularity of the strings is smaller (d$\sim$20 m) in order to have a low energy threshold, since matter effects are maximal at relatively low energies (below 15 GeV). The idea behind these proposals is to map the survival probability of up-going muon neutrinos in (E,cosθ) bins. At energies above $\sim$15 GeV, the oscillation pattern is driven by $\nu_\mu \to \nu_\tau$ vacuum oscillations, while for lower energies some features due to matter enahnced oscillations should appear. As discussed above, this MSW-induced pattern is dependent on mass-hierarchy, namely, it will be present only for neutrinos (anti-neutrinos) if the mass hierarchy is direct (inverse). Fig. 4 shows the expected map of survival probability for muon neutrinos in case of direct or inverse hierarchy. The one for anti-neutrinos is the same, but inverting the two plots.

Neither PINGU nor ORCA have the capability to distinguish ν_μ from $\bar{\nu}_\mu$: therefore, in principle, the sensitivity to mass hierarchy is washed out by the fact that neutrinos behave exactly like anti-neutrinos in the opposite mass-hierarchy hypothesis. However, a measurable net effect remains due to the fact that the (νN) and ($\bar{\nu}$N) cross sections differ significantly in the relevant energy region, $\sigma(\nu\mathrm{N}) \sim 2\sigma(\bar{\nu}\mathrm{N})$, and also the flux of ν_μ is larger than the one of $\bar{\nu}_\mu$. Both PINGU and ORCA estimate to be able of measuring the neutrino mass hierarchy with a 3σ significance after three years of data-taking.

4. Reactor neutrino experiments

Commercial power reactors emit an intense flux of anti-neutrinos ($\sim 2\times10^{20}\ \nu\ \mathrm{sec}^{-1}\ \mathrm{GW}^{-1}$) with a maximum energy of $\sim$ 8 MeV (see Fig. 5, left). Several experiments have exploited this type of neutrinos to study oscillations in disappearance mode with different baselines. The survival probability for $\bar{\nu}_e$ is given by

$$P(\bar{\nu}_e \to \bar{\nu}_e) = 1 - P_{13}(\theta_{13}, \Delta m^2_{13}, \Delta m^2_{23}) - P_{12}(\theta_{12}, \Delta m^2_{12}) \tag{4.1}$$

where

$$\begin{aligned} P_{13}(\theta_{13}, \Delta m^2_{13}, \Delta m^2_{23}) &= \sin^2 2\theta_{13}\left(\cos^2 2\theta_{12}\sin^2\frac{\Delta m^2_{13}L}{4E} + \sin^2 2\theta_{12}\sin^2\frac{\Delta m^2_{23}L}{4E}\right) \\ P_{12}(\theta_{12}, \Delta m^2_{12}) &= \cos^4\theta_{13}\sin^2 2\theta_{12}\sin^2\frac{\Delta m^2_{12}L}{4E} \end{aligned} \tag{4.2}$$

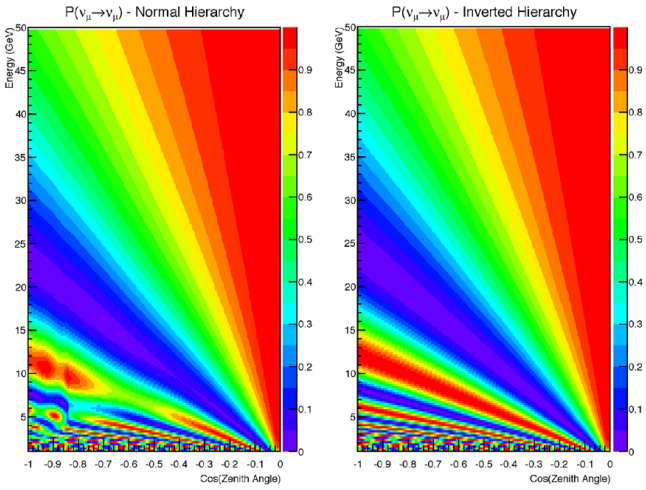

Figure 4: Atmospheric neutrinos. $P(\nu_\mu \to \nu_\mu)$ in bins of energy and zenith-angle in the hypothesis of direct mass hierarchy (left) or inverse mass hierarchy (right). The effect of matter may be recognized for E<15 GeV and is present in the direct mass hierarchy hypothesis only. For $P(\bar{\nu}_\mu \to \bar{\nu}_\mu)$ the two plots are exchanged and the matter effect would be seen in case of inverse mass hierarchy only.

which is effectively divided in two parts: the first one dominates at shorter baselines (L<$\sim$2 Km) and depends mostly on θ_{13}, Δm^2_{13} and Δm^2_{23}; the second one dominates at high baselines (L>$\sim$ 100 Km) and depends mostly on θ_{12}, Δm^2_{12}. For intermediate baselines, both terms contribute. The behaviour of $P(\bar{\nu}_e \to \bar{\nu}_e)$ as a function of the distance from the reactors is shown in Fig. 5, right.

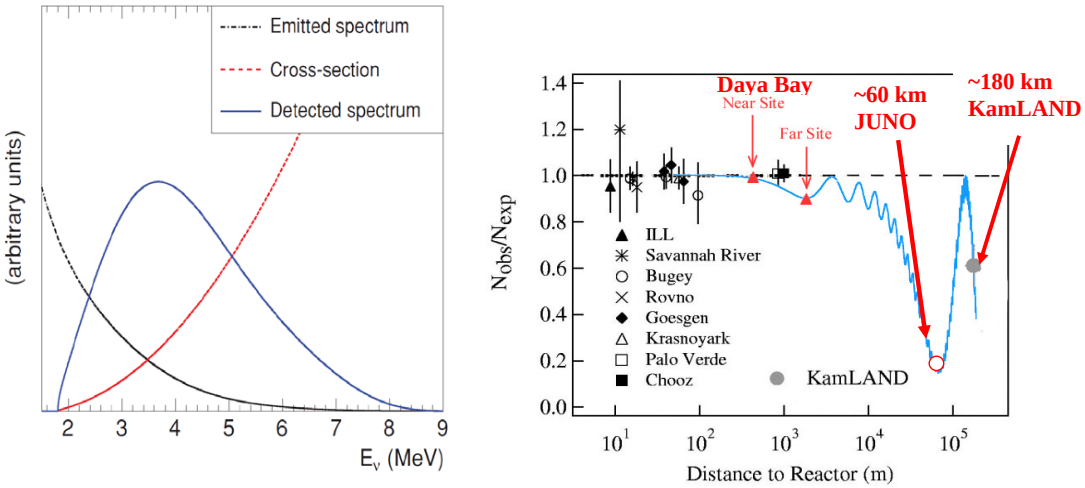

Figure 5: Reactor neutrinos. Energy spectrum (left); $P(\bar{\nu}_e \to \bar{\nu}_e)$ as a function of the distance to reactors (right). The working baselines of the most important experiments are highlighted.

Reactor neutrino experiments detect anti-neutrinos via the inverse beta-decay reaction $\bar{\nu}_e +$

$p \to e^+ + n$ which has a relatively clean signature coming from the coincidence of positron and neutron at a characteristic Δt. This reaction allows them to measure the neutrino energy and therefore to study spectral deformations induced by oscillations.

Long baseline reactor experiments: KamLAND.
KamLAND is a large liquid scintillator experiment (1000 tons of target material) which detects anti-neutrinos coming from reactors located at an average distance of $\sim$180 Km. This long baseline makes it mostly sensitive to θ_{12} and Δm^2_{12}, which are the parameters driving solar neutrinos oscillations (see Section 2). In particular, KamLAND is able of performing a detailed L/E analysis which clearly shows the expected pattern induced by oscillations (see Fig. 6, left). From this, the most stringent constraints on Δm^2_{12} have been extracted [22].

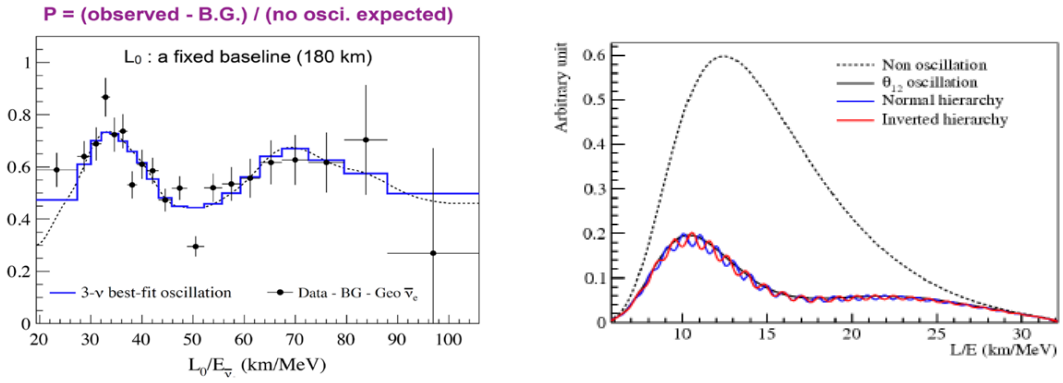

Figure 6: Reactor neutrinos. KamLAND (left): L/E analysis showing a clear pattern of oscillations; Juno (right): L/E pattern expected in the two mass hierarchy hypothesis.

Short baseline reactor experiments: Daya-Bay, RENO, Double-Chooz.
Experiments located at a distance of $\sim$ 1-2 Km from the reactors are in the ideal position to study Δm^2_{13}, and θ_{13}: in fact, in this case the characteristic E/L is of the order of 10^{-3} eV^2, and the contribution of the "solar term"(second term in equation 4.1) to the survival probability is negligible. Therefore, the measured reactor neutrino rate is mostly determined by the first term in equation 4.1 which is driven by $\sin^2 2\theta_{13}$. Note that for the success of these experiments, it is important to keep under control the systematic uncertainties related to the expected flux and spectrum of reactor anti-neutrinos. This is done by building one (or more) Near Detector(s) (L = $\sim$ 300 -500 meters) which measures the characteristics of the unoscillated flux. The first generation reactor neutrino experiments Chooz and Palo Verde had not enough sensitivity to detect the tiny effects due to the first term of eq. 4.1 and were therefore able only to set an upper limits on θ_{13}. The second generation experiments Daya-Bay, RENO and Double Chooz have a significantly improved sensitivity, thanks to their larger masses and better control of systematics. The experiment Daya Bay exploits 8 identical liquid scintillator detectors (20 tons each): 4 of them are located in the far experimental Hall ($\sim$2 Km from the reactor cores), while the remaining 4 are located in two different experimental Halls at distances from the reactor cores ranging between 300 and 500 meters. Daya-Bay

Experiment	Status	E_ν (GeV)	L (Km)	E/L (eV^2)	ν beam	ν type
T2K	Running	0.6	295	2×10^{-3}	KEK-JPARC	ν_μ, $\bar{\nu}_\mu$
MINOS	Completed	2	735	2.5×10^{-3}	Fermilab-NuMi	ν_μ, $\bar{\nu}_\mu$
MINOS$^+$	Running	5	735	6.8×10^{-3}	Fermilab-NuMi	ν_μ, $\bar{\nu}_\mu$
NOVA	Running	2	810	2.5×10^{-3}	Fermilab-NuMi	ν_μ, $\bar{\nu}_\mu$
OPERA	Completed	17	730	2.3×10^{-2}	CERN-CNGS	ν_μ
DUNE	Future	5	1300	3.8×10^{-3}	Fermilab- (new beam)	ν_μ, $\bar{\nu}_\mu$
HYPERK	Future	0.6	295	2×10^{-3}	KEK- (new beam)	ν_μ, $\bar{\nu}_\mu$

Table 2: Accelerator neutrinos. Characteristics of the most important present and future experiments based on accelerator neutrinos.

announced in 2012 the discovery (at 5.2σ) of a non-zero θ_{13} [23]. This result was confirmed later on with a slightly smaller significance by RENO [24] and Double Chooz[25]. More statistics has been accumulated since 2012 and the uncertainty on θ_{13} has been significantly reduced: the most precise value is currently $\sin^2 2\theta_{13}$=0.084±0.005 and comes from the analysis of the full data set of Daya-Bay [26].

The relatively large value of θ_{13} is encouraging for the perspectives of experiments devoted to determine the neutrino mass hierarchy. This is clear for example in case of experiments exploiting resonance in matter, where the term which regulates the effect depends in first place on $\sin^2 2\theta_{13}$ (see expressions 3.1 and 3.2 in the discussion concerning atmospheric neutrinos). It is also true for experiments based on reactor neutrinos (see espression 4.2 in this Section).

Future reactor experiments: JUNO.
Anti-neutrinos from reactors provide an interesting possibility to determine neutrino mass hierarchy, conceptually different from the one discussed in Section 3. The idea is to exploit the interference between the two terms in equation 4.1 with a detector located at an intermediate distance L of $\sim$ 60 Km. The survival probability in this case has wiggles whose position critically depends on the sign of Δm^2_{13} (see Fig. 6, right). In order to be able of distinguishing between the two mass hierarchy hypothesis an excellent energy resolution is therefore required ($\sim 3\%/\sqrt{E}$). This challenging goal is being pursued by the experiment Juno, a huge liquid scintillator detector (20 ktons) under construction in China [27]. Note that in this case mass hierarchy is decoupled from other unknown or poorly known parameters, like δ_{CP} or θ_{23}. This is a clear advantage of this proposal with respect to those based on matter effects (described in Sections 3 and 5).

5. Accelerator neutrino experiments

Intense ν_μ or $\bar{\nu}_\mu$ beams can be obtained artificially at accelerators through the decay of charged pions produced by protons impinging on a dedicated target. Several present and future long-baseline experiments exploit these beams to study both $\nu_\mu \to \nu_e$ appearance and ν_μ disappearance. A summary of their characteristic parameters (neutrino energy, baseline, current status) is shown in table 2. All experiments (with the exception of OPERA) have L/E centered on 10^{-3} eV^2 and are therefore optimized to study oscillations driven by the squared mass difference Δm^2_{13}.

OPERA has worked with a higher neutrino energy (and therefore E/L is centered around $10^{-2}\,\mathrm{eV}^2$), because its main goal was to observe $\nu_\mu \to \nu_\tau$ appearance. In fact, in this case a minimum threshold energy of $\sim 3.5\,\mathrm{GeV}$ is needed in order to detect ν_τ by τ lepton production. OPERA reconstructs the topology of the neutrino interactions thanks to 150000 bricks of nuclear emulsions arranged in two super-modules. They first observed a ν_τ event in 2010. Since then, four more events have been detected leading to the discovery of ν_τ appearance with a significance of 5σ [28].

The probabilty for $\nu_\mu \to \nu_e$ appearance in LBL experiments has a complicated dependency from all the relevant oscillation parameters and is also influenced by matter effects, as can be seen in expression 5.1 (to 1^{st} order approximation in matter effect) [29]

$$\begin{aligned} P(\nu_\mu \to \nu_e) = {} & c_{13}^2 s_{13}^2 s_{23}^2 \cdot \sin^2\Delta_{13} \\ & + 8c_{13}^2 s_{12} s_{13} s_{23} \left(c_{12} c_{23} \cdot \cos\delta_{CP} - s_{12} s_{13} s_{23}\right) \cdot \cos\Delta_{32} \cdot \sin\Delta_{31} \cdot \sin\Delta_{21} \\ & - 8c_{13}^2 c_{12} c_{23} s_{12} s_{13} s_{23} \cdot \sin\delta_{CP} \cdot \sin\Delta_{32} \cdot \sin\Delta_{31} \cdot \sin\Delta_{21} \\ & + 4s_{12}^2 c_{13}^2 \left(c_{12}^2 c_{23}^2 + s_{12}^2 s_{23}^2 s_{13}^2 - 2c_{12} c_{23} s_{12} s_{23} s_{13} \cos\delta_{CP}\right) \cdot \sin^2\Delta_{21} \\ & - 8c_{13}^2 s_{13}^2 s_{23}^2 \cdot \frac{\alpha \mathrm{L}}{4\mathrm{E}_\nu} \left(1 - 2s_{13}^2\right) \cdot \cos\Delta_{32} \cdot \sin\Delta_{31} \\ & + 8c_{13}^2 s_{13}^2 s_{23}^2 \cdot \frac{\alpha}{\Delta \mathrm{m}_{13}^2} \left(1 - 2s_{13}^2\right) \cdot \sin^2\Delta_{31} \end{aligned} \tag{5.1}$$

where

$$\Delta_{ij} = \frac{\Delta \mathrm{m}_{ij}^2 \mathrm{L}}{4\mathrm{E}_\nu}; \alpha = 2\sqrt{2}\mathrm{G}_F n_e \mathrm{E}_\nu = 7.56 \times 10^{-5}[\mathrm{eV}^2] \times \rho[\mathrm{g/cm}^3] \times \mathrm{E}_\nu[\mathrm{GeV}]$$

The corresponding probability for $\bar{\nu}_\mu \to \bar{\nu}_e$ can be obtained by replacing $\delta_{CP} \to -\delta_{CP}$ and $\alpha \to -\alpha$. Long baseline experiments which are able of detecting ν_e appearance, like T2K, are sensitive to θ_{13} as can be seen from the leading term in expression 5.1 (first term). However, the dependency of the oscillation probability from θ_{13} is complicated by the presence of other unknowns, like δ_{CP}, mass hierarchy or θ_{23} octant, which makes this measurement less straightforward with respect to the one performed with reactor experiments (see Section 4). The third term in expression 5.1, dependent on $\sin\delta_{CP}$, is responsible for CP violation since changes sign going from ν_μ to $\bar{\nu}_\mu$. The last two terms, dependent on α, describe the contribution of matter effects to the oscillation probability. As seen also in Section 3, the matter terms have opposite sign for different mass hierarchy conditions and for ν_μ and $\bar{\nu}_\mu$. The complicated interplay between different unknown quantities creates a certain degree of ambiguity in the interpretation of ν_e appearance data. For example, the difference between ν_e and $\bar{\nu}_e$ appearance which is present because of matter effects can mask the true CP violating contribution coming from δ_{CP}. Also, the effect depends on mass hierarchy, which is currently unknown. The complexity of the situation can be clearly appreciated in the example of Fig. 7, where ν_e ($\bar{\nu}_e$) appearance probability is shown (for L=295 Km) for different values of δ_{CP} and different hypothesis on mass hierarchy.

The results on ν_e appearance can be complemented by studies on ν_μ disappearance.

$$P(\nu_\mu \to \nu_\mu) \simeq \sin^2 2\theta_{23} \sin^2\left(\frac{\Delta \mathrm{m}_{32}^2 \mathrm{L}}{4\mathrm{E}_\nu}\right) \tag{5.2}$$

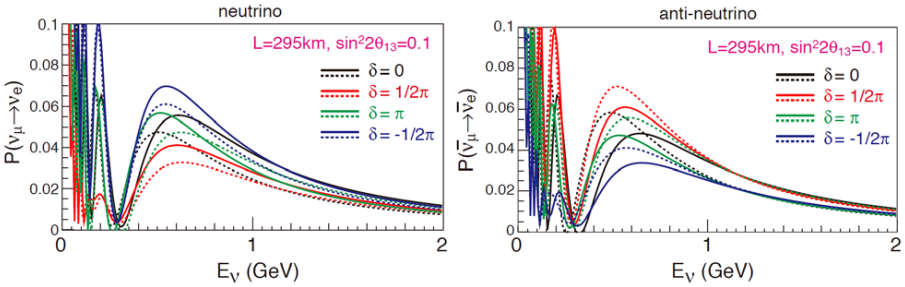

Figure 7: Accelerator neutrinos: ν_e ($\bar{\nu}_e$) appearance probability (for L=295 Km) for different values of δ_{CP} and different hypothesis on mass hierarchy (NH: solid lines; IH: dashed lines).

The first indication of $\nu_\mu \rightarrow \nu_e$ appearance was published by T2K in 2011. T2K exploits a ν_μ beam produced at the J-PARC facility (Japan) and directed toward the Super-Kamiokande detector, 295 Km away. Super-Kamiokande is slightly off-axis with respect to the beam direction ($\sim 2.5°$) in order to select a relatively small range of neutrino energies (peaked at 0.6 GeV). After a total exposure of $6.57\times\ 10^{20}$ POT, corresponding to data taken between 2010 and 2013, T2K has collected 28 ν_e candidates with $\sim$5 events expected from background, and has published evidence of electron neutrino appearance with a significance of 7.5σ [30]. The value of θ_{13} derived from this measurement is slightly higher with respect to the one reported by reactor experiments. This small tension may be accomodated with a non-zero value of δ_{CP}: a combined fit to reactor experiments and T2K slightly favours $\delta_{CP}=\pi/2$. T2K has also observed ν_μ disappearance from which the best measurement of θ_{23} has been extracted: $\sin^2\theta_{23} = 0.514^{+0.055}_{-0.056}$ (normal hierarchy), $\sin^2\theta_{23} = 0.511^{+0.055}_{-0.055}$ (inverse hierarchy) [30]. T2K has recently started running with a $\bar{\nu}_\mu$ beam: the results are consistent with the one obtained with ν_μ although the statistics is still too low to draw definite conclusions [31].

The most precise measurement of Δm^2_{23} (uncertainty of 4%) comes from the long baseline MINOS experiment which studies ν_μ disappearance with a 2-5 GeV neutrino beam shot from Fermilab to the Soudan mine 735 Km away [32].

NOνA is a liquid scintillator experiment which also exploits a ν_μ beam produced at the Fermilab NuMi facility. It started taking data recently in the complete configuration (2014) and is expected to produce physics results soon. NOνA and T2K have similar E/L, but significantly different E and L, so the contributions to the oscillation probability coming from the various terms in expression 5.1 have different weights (for example, matter effects are much more important in NOνA than in T2K). This makes the two experiments complementary and the combined analysis of the two data-sets will be important to break degeneracy between the unknown quantities.

Future accelerator neutrino experiments: DUNE and HYPERK.
Even though it is possible that the combined results of currently running experiments will soon start to provide some hints towards the solution of the neutrino puzzle, more statistics and better control of systematics will be needed to shed light on all the missing details. This will be provided by the next generation experiments, DUNE [33] and HyperK [29], which are being designed with the goal of collecting large samples of events both in appearance ($\sim$ 1000 events) and disappearance

($\sim$ 10000 events) mode. DUNE will be a 40 kton LAr TPC located at the Sanford Underground Laboratory, in the Homestake Mine, 1300 Km from Fermilab. It will detect neutrinos from a very intense $\nu_\mu/\bar{\nu}_\mu$ beam with <E>$\sim$5 GeV. HyperK will be a huge Cerenkov detector, 25 times bigger than Super-Kamiokande, located at $\sim$300 Km from the JPARC-KEK facility. Like in T2K the detector will be off-axis with respect to the beam direction and will have an energy centered around 0.6 GeV. The two future LBL projects are highly complementary: they have different baselines and are therefore influenced by matter effects in different ways. They have different systematics associated to the detecting techniques (LAr and water Cerenkov) and different types of beam background (DUNE is on-axis, while HyperK is off-axis). For this reason, both experiments are an important part of the global strategy to complete the neutrino puzzle.

6. Conclusions and outlook

Since the first discovery of neutrino oscillations in 1998, many parts of the neutrino puzzle have been completed. A rich experimental program is being developed to determine the pieces which are still missing: the synergy between different experiments will be a crucial element to break degeneracies and reduce the impact of systematic errors. For favourable combinations of the parameter values we may have indications on mass hierarchy and δ_{CP} already with the current generation of experiments (T2K, NOνA). In any case, the wealth of data which will come from future experiments (JUNO, RENO-50, INO, PINGU, ORCA, HYPERK, DUNE) will allow precise determination of all the missing pieces and significant improvement on the already known parameters.

References

[1] B. Pontecorvo, JETP **7**, 172 (1958); B. Pontecorvo, JETP **6**, 429 (1958).

[2] Y. Fukudae et al. (Super-Kamiokande Collaboration), Phys. Rev. Lett. **81**, 1562 (1998).

[3] Q.R. Ahmad et al. (SNO Collaboration), Phys. Rev. Lett. **89**, 011301 (2002).

[4] "Experimental Neutrino Physics 2: SBL, β-decay, neutrinoless $\beta\beta$-decay", contribution from Juan Jose Gomez Cadenas (EPS-HEP 2015, Vienna).

[5] C. Albright et al. (Neutrino Factory, Muon Collider Collaboration), arXiv:physics/0411123v2.

[6] R. Davis, D.S. Harmer, and K.C. Hoffman, Phys. Rev. Lett. **20**, 1205 (1968); B.T. Cleveland et al. (Homestake Collaboration), Astrophys. J. **496**, 505 (1998).

[7] W. Hampel et al. (GALLEX Collaboration), Phys. Lett. B **447**, 127 (1999); M. Altmann et al. (GNO Collaboration), Phys. Lett. B **490**, 16 (2000).

[8] J.N. Abdurashitov et al. (SAGE Collaboration), JETP **95**, 181 (2002).

[9] Y. Fukuda et al. (Super-Kamiokande Collaboration), Phys. Rev. Lett. **81**, 1158 (1998).

[10] B. Aharmim et al. (SNO Collaboration) Phys. Rev. C **88**, 025501 (2013).

[11] G. Alimonti et al. (BOREXino), NIM A **600**,568 (2009); G. Bellini et al. (BOREXino), Phys.Rev. D, **89**, 112007 (2014).

[12] A. Serenelli et al. *Astrophys. J.*, **743**, 24 (2011).

[13] Atsuto Suzuki, arXiV:1409.4515; M. C. Gonzalez-Garcia, M. Maltoni, T. Schwetz, arXiV: 1409.5439.

[14] G. Bellini et al. (BOREXino), Nature, **512**, 383 (2014).

[15] A. Palazzo, arXiV:1101.3875; M. C. Gonzalez-Garcia, M. Maltoni, arXiV:1307.3092; P. C. de Holanda, A. Yu. Smirnov, arXiV:1012.5627.

[16] K. S. Hirata et al. (Kamiokande-II Collaboration), Phys.Lett. B **205**, 416 (1988); Phys.Lett. B **280**, 146 (1992).

[17] D. Casper et al., Phys.Rev.Lett. **66**, 2561 (1991); R. Becker-Szendy et al., Phys.Rev. D **46**, 3720 (1992).

[18] K Abe et al. (Super-Kamiokande Collaboration), Phys.Rev.Lett. **110**, 181802 (2013).

[19] Majumder Gobinda, "Status and perspectives of India based neutrino observatory (INO)", Talk at the XVI International Workshop on Neutrino Telescopes, Venice, March 4^{th} 2015.

[20] O. Mena et al., Phs.Rev. D **78**, 093003 (2008); LoI of PINGU, arXiV:1401.2046.

[21] U. F. Katz (for the KM3NET Collaboration), arXiV:1402.1022, Proceedings of the XV Workshop on neutrinos telescopes, Venice, March 11^{th} 2013.

[22] S. Abe et al. (KamLAND Collaboration), Phys.Rev.Lett. **100**, 221803 (2008).

[23] F. P. An et al. (Daya Bay Collaboration), Phys.Rev.Lett. **108**,171803 (2012).

[24] J.K. Ahn et al. (RENO Collaboration), Phys.Rev.Lett. **108**, 191802 (2012).

[25] Y. Abe et al. (Double Chooz Collaboration), Phys.Rev.D **86**, 052008 (2012).

[26] "Recent progress from Daya Bay", contribution from Xiangpan Ji (EPS-HEP 2015, Vienna); arXiv:1505.03456.

[27] T. Adam et al (Juno Collaboration) arXiv:1508.07166.

[28] N. Agafonova et al. (OPERA Collaboration), Phys.Rev.Lett. **115**, 121802 (2015).

[29] K. Abe et al. ArXiV:1502.05199; J. Arafune, M. Koike, and J. Sato, Phys. Rev., D **56**, 3093 (1997).

[30] K. Abe et al (T2K Collaboration) Phys.Rev.Lett. **112**, 061802 (2014); K. Abe et al (T2K Collaboration) Phys.Rev.Lett. **112**, 181801 (2014).

[31] "New anti-neutrino oscillation results from T2K", Talk at the EPS Conference on High Energy Physics, Vienna 22-29 July 2015. EPS-HEP, Vienna by M. R. Salzgeber)

[32] P. Adamson et al. (MINOS Collaboration), Phys.Rev.Lett. **112**, 191801 (2014).

[33] https://web.fnal.gov/project/LBNF/SitePages/Home.aspx, 2014.